[6] Spalding, D. B., "The Combustion of Liquid Fuels," *4th Symposium (International) on Combustion*, The Combustion Institute, Pittsburgh, Pa., pp. 847–864.

[7] Ingebo, R. D., "Photomicrographic Tracking of Ethanol Drops in a Rocket Chamber Burning Ethanol and Liquid Oxygen," TN D-290, 1960, NASA.

[8] Campbell, D. T. and Chadwick, W. D., "Combustion Instability Analysis at High Chamber Pressure," AFRPL-TR-68-179, 1968, Air Force Rocket Propulsion Lab., Wright-Patterson Air Force Base, Ohio.

[9] Rabin, E. A. et al., "The Motion and Shattering of Propellant Droplets," AFOSR TN-60-59, 1960, Air Force Office of Scientific Research, Wright-Patterson Air Force Base, Ohio.

[10] Eisenklam, S. A. et al., "Evaporation Rates and Drag Resistance on Burning Drops," *11th Symposium (International) on Combustion*, The Combustion Institute, Pittsburgh, Pa., 1966, pp. 715–728.

[11] Kumagai, S. and Isoda, H., "Combustion of Fuel Droplets in a Falling Chamber," *The 6th Symposium (International) on Combustion*, The Combustion Institute, Pittsburgh, Pa., 1956, pp. 726–731.

[12] Nuruzzaman, A. S. M., Hedley, A. B., and Beer, J. M., "Combustion of Monosized Droplet Streams in Stationary Self-Supporting Flames," *13th Symposium (International) on Combustion*, The Combustion Institute, Pittsburgh, Pa., 1970, pp. 787–799.

[13] Bracco, F. V., "An Experimental-Analytical Method to Study Steady Spray Combustion," *Journal of Spacecraft and Rockets*, Vol. 10, No. 6, June 1973, pp. 353–354.

NOVEMBER 1974 AIAA JOURNAL VOL. 12, NO. 11

Steady, Incompressible, Swirling Jets and Wakes

ARTUR MAGER*
The Aerospace Corporation, El Segundo, Calif.

The problem of steady, incompressible, swirling, laminar, or turbulent jets and wakes, with their surroundings either in axial motion or at standstill, is formulated in the plane of parameters characteristic of the axial and circumferential velocities. This permits one to discern the physically realistic cases and allows an insight into the behavior of the solutions, particularly near the discontinuities. Examples of continuous (some in closed form) and discontinuous solutions for wakes and jets are given. These show that the axial motion of the surroundings reduces the flow expansion and that the swirling wakes behave quite differently from swirling jets. Good agreement with the available analytical and experimental work of others on swirling jets in still surroundings is indicated.

Introduction

THE method, previously proposed by the author for the study of vortex cores,[1] is extended here to swirling, unbounded flows without net circulation when their surroundings are either in axial motion or at a standstill. These flows are of practical interest because they represent idealizations of real flow situations occurring downstream from propellers, turbojets, air turbines, windmills; and in certain sprays, atomizers and combustion chambers, as well as in models of such natural phenomena as dust devils and water spouts.

In spite of this wide applicability, flows of this kind have received but little attention. Only the swirling jets which issue into still surroundings have been extensively studied analytically and experimentally.[2–10] A review of the analyses reveals that two are quasi-empirical,[4,5] others are restricted to apply when the pressure varies in the axial direction only,[3,9] still others are limited by their experimentally determined constants to certain specific values of the initial swirl[5,10] or by the form and number of the computed expansion terms to conditions away from the origin where the flow is but slightly different from the nonswirling flow.[2] None applies in regions where the swirl is high enough to cause flow reversal. But reversed flows and initial enlargement of the jet's diameter close to the exit nozzle have been observed in such flows by many investigators[5,7,8] and from the practical standpoint of rapid mixing and dispersion they are precisely the features which are most interesting. Therefore, one would like to understand the conditions which lead to such an irregular behavior. This state of knowledge is even more meager when the flow surroundings are in axial motion. To the best knowledge of the author only one experimental investigation of swirling wake has been reported in the literature[11] and the available analytical solutions[11–15] are either limited to weakly swirling far downstream regions[11,12] or apply exclusively to wakes only. For the most part these solutions are continuous and though Gartshore[14] suggested that the discontinuities that he encountered may be the analytical counterpart of the sometimes seen vortex breakdown, he failed to pursue this idea to its full potential. But it is the breakdown of the flow which is perhaps the most interesting feature of swirling wakes because without it, such wakes tend to diffuse very slowly, persisting for long distances behind the generating body—a situation which is often undesirable.

To understand the nature of the solutions, Gartshore[15] plotted their trajectories in a phase plane, that is in the plane of the parameters characteristic of the axial and circumferential velocities, but for some reason he never made the connection between the trajectories and his on-axis condition thus failing to see how the discontinuities arise. Nevertheless, it is this plot of Gartshore's that suggested to the author the method of Ref. 1 which, for flows with circulation, not only afforded a clear insight into the behavior of the solutions close to the discontinuities and at the downstream infinity, but also showed in the case of multiple branch solutions, how crossovers from one branch to another may happen. One would thus expect that the application of this same method to swirling wakes and jets will also permit, in addition to their normal viscous dissipation, the determination of the conditions which lead to their very interesting, irregular behavior.

Phase Plane

Using the quasi-cylindrical approximation, denoting all dimensional quantities by an overbar and dividing all velocities

Presented as Paper 74-35 at the AIAA 12th Aerospace Sciences Meeting, Washington, D.C., January 30–February 1, 1974; submitted February 11, 1974; revision received June 10, 1974.

Index category: Jets, Wakes, and Viscid-Inviscid Flow Interaction.

* Vice President and General Manager, Engineering Science Operations. Fellow AIAA.

by the maximum velocity $\bar{Q} \equiv (2\bar{P}_\delta/\bar{\rho})^{1/2}$, all pressures by the maximum dynamic pressure $0.5\bar{\rho}\bar{Q}^2$ (so that the nondimensional external total pressure P_δ is unity) and all lengths by the initial swirling flow boundary $\bar{\delta}_i$, one writes in cylindrical coordinates (r, θ, z) with corresponding velocity components (u, v, w) the integrated momentum-integral equations for steady, incompressible, laminar or turbulent flow without net circulation (for derivation see Ref. 1) as

$$p_o = 1 - W^2 - I_3; \quad I_{11} + 0.5I_{22} = \kappa_1; \quad I_{12} = \kappa_2 \text{ (1a, b, c)}$$

where subscript o denotes conditions on the axis, p is the absolute static pressure and for turbulent flow mean quantities are used.

In these equations it was assumed that at the boundary of the swirling flow the axial velocity w attains a constant, known value W, the circumferential velocity v vanishes and the various integrals are defined as

$$I_{11} \equiv \int_0^\delta (W-w)wr\,dr; \quad I_{22} \equiv \int_0^\delta v^2 r\,dr; \quad I_{12} \equiv \int_0^\delta vwr^2\,dr;$$

$$I_3 \equiv 2\int_0^\delta (v^2/r)\,dr$$

so that the constants κ_1 and κ_2 are the flow force deficiency and the axial flux of the angular momentum, respectively.

It is obvious that alone, Eqs. (1a–c) are not capable of describing the dissipation of the swirling flow because they are independent of the axial distance z. An additional relation is required and it is obtained by taking the limit of the statement of the conservation of momentum in the axial direction [e.g., Eq. (1d) of Ref. 1] as $r \to 0$:

$$(dP_o/dz) = (4W/Re)w_{rr}(0) \qquad \text{(1d)}$$

where $Re \equiv \bar{W}\bar{\delta}_i/\bar{\nu}$ is the Reynolds number.†

The various integrals $I_{11}, I_{12}, I_{22}, I_3$ are related to each other and to the flow area $a(=\delta^2)$, as well as to the static pressure p_o, by specifying the velocities v and w using slightly modified expressions of Refs. 13 and 15

$$w = W[\alpha + (1-\alpha)f_1]; \quad v = W\beta f_2 \qquad (2)$$

where

$$f_1 \equiv \eta^2(6 - 8\eta + 3\eta^2); \quad f_2 \equiv 4\eta[\tfrac{4}{3}(1-\eta)]^3; \quad \eta \equiv r/\delta$$

and $\alpha \equiv w_o/W$ is the form parameter of the axial velocity distribution, while $\beta \equiv V/W$ is the form parameter of the circumferential velocity distribution whose maximum value is given by $V = v(\frac{1}{4})$.

The above expressions, describing fully developed flow, allow the velocities in the swirling region to match the magnitudes and the slopes of their corresponding components ($w = W$; $v = 0$) in their surroundings and set the curvature of the axial velocity on the centerline to equal $w_{rr}(0) = 12W(1-\alpha)/a$. Because of this connection, when $\alpha > 1$ (e.g., for jets) the velocity profile is always convex, while for wakes ($\alpha < 1$) the velocity profile is always concave. The above expressions also imply a similarity of the axial velocity-deficiency profile and the circumferential velocity profile which, while known to exist for nonswirling wakes and jets, have been experimentally demonstrated only in the case of swirling jets in still surroundings.[5,6] Our expressions, of course, fit these experimental data reasonably well.

Using the so postulated expressions for the velocities the integrals may be written as

$$I_{11} = aW^2F_1; \quad I_{12} = a^{3/2}W^2\beta F_2; \quad I_{22} = aW^2\beta^2 C_3;$$

$$I_3 = 2W^2\beta^2 C_6$$

where $F_j \equiv K_{j0} + K_{j1}\alpha + K_{j2}\alpha^2$ with the constants C_i and the coefficients K_{ji} listed in the Appendix, so that Eqs. (1a–d) become

$$P_o = p_o + w_o^2 = 1 - W^2(1 - \alpha^2 + 2C_6\beta^2) \qquad (3a)$$

$$\kappa_1 = aW^2(F_1 + 0.5C_3\beta^2) \qquad (3b)$$

$$\kappa_2 = a^{3/2}W^2F_2\beta \qquad (3c)$$

† For turbulent flow, the kinematic viscosity $\bar{\nu}$ is replaced by the eddy diffusivity $\bar{\nu}_t$.

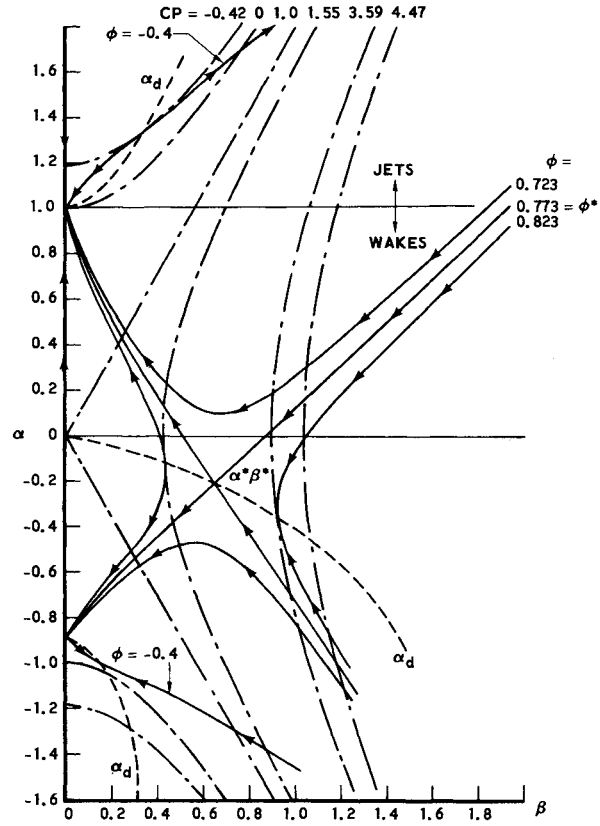

Fig. 1 Phase plane for wakes and jets in steady external stream.

$$0.5aP_o' = a(\alpha\alpha' - 2C_6\beta\beta') = 1 - \alpha \qquad (3d)$$

where the dashes denote total differentiation with respect to $\zeta \equiv 24z/Re$.

Equations (3a–d) are sufficient to determine the four unknown quantities $\alpha(\zeta)$, $\beta(\zeta)$, $a(\zeta)$, and $P_o(\zeta)$ when W is known and the constants κ_1 and κ_2 are obtained from the initial values α_i, β_i.‡ To examine the trajectories of such solutions we follow the approach of Gartshore[15] and eliminate the flow area a between Eqs. (3b) and (3c). Setting $\phi \equiv \kappa_1/(\kappa_2 W)^{2/3}$ we thus obtain a single equation

$$F_1 + 0.5C_3\beta^2 - \phi(F_2\beta)^{2/3} = 0 \qquad (4)$$

whose solutions for a given ϕ satisfy not only the axial (as in Ref. 1), but also the circumferential momentum-integral equation. These solutions are plotted in the $\alpha - \beta$ plane known as the phase plane (Ref. 1).§ Such a plot for a number of values of ϕ is shown in Fig. 1. As may be seen from this figure, these curves are remarkably similar to those obtained in Ref. 1 for constant flow force deficiency and there is a singular value of $\phi = \phi^* = 0.7732$ (for derivation see Ref. 16) which divides the solutions of Eq. (4) into those which exist for all β and those which do not. Each one of these is double branched but for $\phi = \phi^*$ all the branches join at the singular point $\alpha^* = -0.2094$, $\beta^* = 0.6436$. This similarity to the results of Ref. 1 occurs because, physically, ϕ is also a measure of the flow force deficiency but taken relative to the $\frac{2}{3}$ power of the axial flux of the angular momentum.

Having thus obtained the trajectories of Eq. (4), it is next necessary to connect these with the axial distance ζ. In Ref. 1 this could be conveniently done because the lines of constant ζ were given by the solution of the angular momentum equation. Here, however, Eq. (3d) cannot be integrated in a closed form so that

‡ Because of nondimensionalization, the initial value a_i is always unity.

§ In Ref. 1, the plane $\alpha - R$ is called the phase plane with $R \approx \beta^2$. However, this slight difference appears to be unimportant.

its integration must be performed for each value of ϕ along the particular trajectory of Eq. (4). Nevertheless, it is apparent from the form of Eq. (3d) that for wakes (e.g., $\alpha < 1$) the total pressure P_o must increase in the downstream direction. Conversely, Eq. (3d) also shows that for jets (e.g., $\alpha > 1$) P_o must decrease in the downstream direction. Since the lines of constant P_o may easily be computed from Eq. (3a), one is thus able to study in a qualitative manner the behavior of the solutions for wakes and jets in spite of the fact that Eq. (3d) is nonintegrable. To this end, some of the representative CP lines were plotted in Fig. 1. [Since $CP \equiv (1-P_o)/W^2$, P_o increases whenever CP decreases and vice versa.]

Thus, by following the intersections of the CP lines with the ϕ lines in the direction of P_o increasing or decreasing one is able to trace the course of the solutions for wakes or jets, respectively. However, it should be noted that while such a procedure may be expected to give good insight into the nature of the solutions, particularly near discontinuities, the actual dependence on ζ must still be obtained by the integration of Eq. (3d) along a constant ϕ line. Since along such a line $\alpha(\beta)$ is known and $a(\beta)$ may be obtained from Eq. (3b)

$$a = [F_1(\alpha_i) + 0.5C_3\beta_i^2]/[F_1 + 0.5C_3\beta^2] \tag{5}$$

therefore this integration may easily be performed numerically by evaluating

$$\zeta = \zeta_i + \int_{\beta_i}^{\beta} \{[a(\alpha D - 2C_6\beta)]/(1-\alpha)\}\, d\beta \tag{6}$$

where $D \equiv d\alpha/d\beta$ is the ϕ line slope[16] and subscript i denotes the initial conditions.

Swirling Wakes

Continuous Solutions

Consider $\phi < \phi^*$ and $\alpha < 1$. For such conditions we see from Fig. 1 that the double-branched solutions of Eq. (4) exist for all values of β, passing at $\beta = 0$ through $\alpha = 1$ and $\alpha = -\frac{10}{11}$. But since for wakes, P_o must increase in the downstream direction, it is obvious from Fig. 1 that the wake solutions for $\phi < \phi^*$ are obtained at the intersection of the CP and ϕ curves moving continuously in the direction of decreasing β. Furthermore, since the upper branches of the ϕ curves all terminate at $\alpha = 1$, Eq. (6) shows that the point $\alpha = 1$, $\beta = 0$ represents the downstream infinity with $w = W$, $v = 0$, $p_o = p_\delta = 1 - W^2$ and $P_o = P_\delta = 1$, as expected. By the same token the lower branches, which at $\beta = 0$ reach their maximum value of P_o but yield there a strongly reversed flow on the axis, do not represent physically realistic solutions for swirling wakes.¶ This situation is very similar to that found for continuous solutions of vortex cores in Ref. 1 and this similarity is even more apparent in Figs. 2a–c where the results obtained by solving Eq. (6) are plotted for $\alpha_i = 0.6$ and various values of β_i. As in vortex cores, with increasing axial distance the circumferential velocity is steadily reduced but the axial flow on the axis is first decelerated to some minimum value and only then accelerated. In fact, for strong enough initial swirl, Fig. 2a shows this deceleration to cause a small region of reversed flow on the axis. The physical reasons for this process were explained in Ref. 1 and will not be repeated here. Also, as may have been expected, these results are in good agreement with those obtained in Refs. 13–15 whose authors have used but a slightly different integration process. Of greater practical interest, however, is the behavior of swirling wakes at fixed ζ. As may be seen from Figs. 2b and 2c, with increasing initial swirl the swirling wakes tend to become more slender and this, of course, delays the dissipation of the swirling flow. Furthermore, as seen from Fig. 2a, increasing swirl also delays the axial velocity recovery. Thus for high enough swirl, one may expect the swirling wakes, just like the vortex cores, to persist for long distances behind the generating body.

Very far downstream, where the swirling flow is nearly dissipated, swirling wakes should behave like the nonswirling wakes. Indeed, by setting $\beta = 0$ in Eqs. (3a–d) one obtains

$$a = F_{1i}/F_1; \quad a\alpha\alpha' = 1 - \alpha \tag{7}$$

which integrates with $\zeta_i = 0$ and

$$\theta_1 \equiv \tfrac{11}{21}\{[1/(1-\alpha)] - (10/21)\ln|[\alpha + (10/11)]/(1-\alpha)|\}$$

to

$$\zeta = (F_{1i}/K_{12})(\theta_{1i} - \theta_1) \tag{8}$$

This solution is shown in Figs. 2a and c where it indicates that the effects of swirl on wakes tend to persist quite far downstream.

Finally since, for a fixed α_i, the increasing β_i implies an increasing relative flow force deficiency ϕ, it is obvious from Fig. 1 that results analogous to those shown in Figs. 2a–c, may also be obtained for a fixed β_i but with a decreasing α_i.

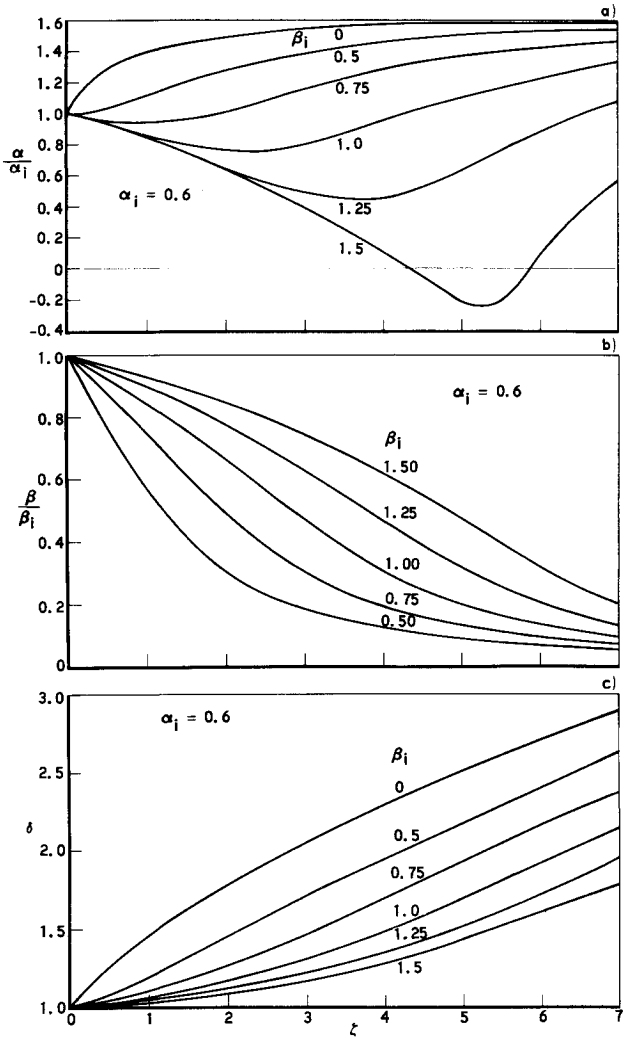

Fig. 2 Effect of swirl on wakes: a) axial velocity on the axis; b) maximum circumferential velocity; c) flow boundary.

Discontinuous Solutions

As may be seen in Fig. 1, when $\phi = \phi^*$, the upper and lower branches of the solutions of Eq. (4) are joined at the point α^*, β^* and then, for $\phi > \phi^*$, they remain joined; but there appears a region of β, on both sides of β^*, in which these solutions do not exist. Thus, by examining Fig. 1, one sees that tracing the intersections of the CP lines with the ϕ lines in the direction of decreasing CP when $\phi > \phi^*$ must eventually lead to a point where the CP curve is tangent to the ϕ curve and beyond which these intersections cannot continue so that the solution of Eqs. (3a–d) disappears.

This process is again very similar to that described for vortex cores in Ref. 1 where, following Hall,[17] the disappearance of

¶ Except, of course, for some piecewise solutions which may be required to fit a special set of downstream conditions.

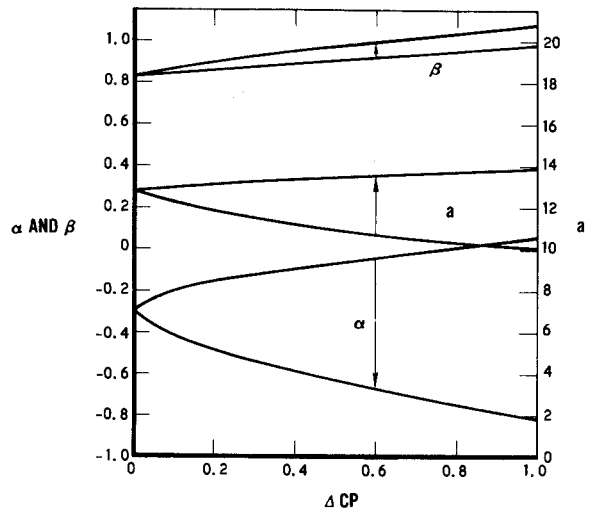

Fig. 3 Crossover changes upstream of spiral breakdown for $\phi = 0.798$.

these quasi-cylindrical flow solutions was identified with the initiation of the so-called asymmetrical spiral breakdown, which has been so vividly photographed by Sarpkaya[18] and others. More recently, the validity of such an identification in divergent tubes has been experimentally demonstrated by Sarpkaya.[19] Thus, it is important to determine the locus $\alpha_d(\beta_d)$ of such tangency points. This is done by equating the slopes of the P_o and ϕ curves.[16] The solution has a central branch which falls into the region of wake flows and passes through the point α^*, β^*. The spiral breakdown will thus occur for all $\phi > \phi^*$ and $\beta_i > \beta_i^*$ ** but only when the values of α_d and β_d given in Fig. 1 are reached.

For vortex cores, as discussed in Ref. 1, when the flow ahead of the spiral breakdown is on the upper branch (e.g., above the α_d line) it may cross to the lower branch along the line of constant ζ (which for those flows is also the line of constant angular momentum). Such crossovers have been shown to be completely equivalent to the finite transitions studied by Benjamin[20] and appear to be the analytical counterpart of the axisymmetric bubbles which are sometimes observed[18] ahead of the spiral breakdown. Of course, for swirling flows without net circulation these crossovers, if and when they occur, may be expected to follow the line of constant P_o because, according to Eq. (3d) when $dP_o = 0$, $d\zeta$ must also vanish. Thus, to indicate the effect that such crossover may cause, the behavior of α, β and a along the two branches of the $\phi = 0.798$ line is plotted in Fig. 3 at the same values of $\Delta CP \equiv (P_{o,d} - P_o)/W^2$. To see the changes one simply moves in this figure, as indicated by the arrows, at a constant value of ΔCP. In this way we observe that, close to the discontinuity, the behavior of the wake solution is again qualitatively similar to that described in Ref. 1 for vortex cores.

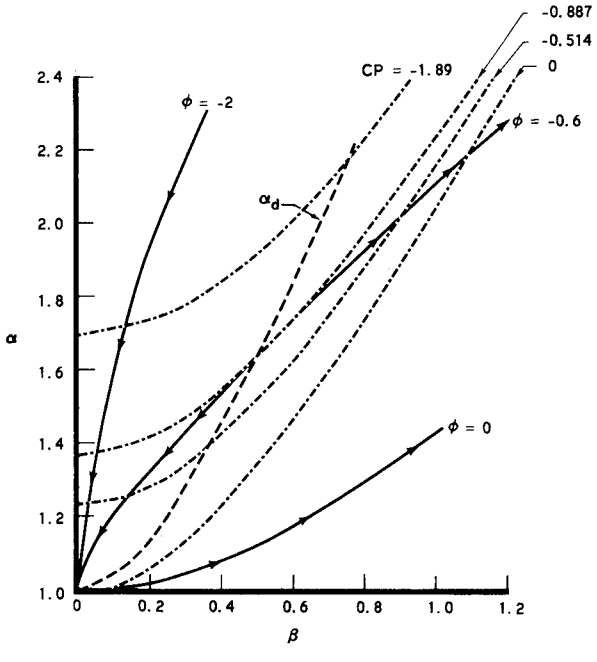

Fig. 4 Phase plane for jets in steady external stream.

** For $\phi > \phi^*$ and $\beta_i < \beta^*$ the solutions will be continuous.

Swirling Jets

Continuous Solutions

Jets have a flow force greater than their surroundings so that one may expect κ_1 and ϕ to be negative. This excess flow force is greatest when $\phi \to -\infty$ and $\beta = 0$ is the corresponding ϕ line. However, as the excess of the flow force decreases, e.g., as $\phi \to 0$, the constant ϕ lines all intersect the upper branch of the $\alpha_d(\beta_d)$ line. This is shown in Fig. 4 where that region of Fig. 1 which is appropriate for swirling jets is plotted in detail. As may be seen from this figure the solutions for all swirling jet flows may encounter discontinuities and the swirl at which this will happen is proportional to the excess of the flow force.

Now consider those flows for which at any $\alpha_i, \beta_i < \beta_d$ (say along $\phi = -2.0$ line). Since for $\alpha > 1$ the total pressure P_o must decrease (e.g., CP must increase) in the downstream direction, it

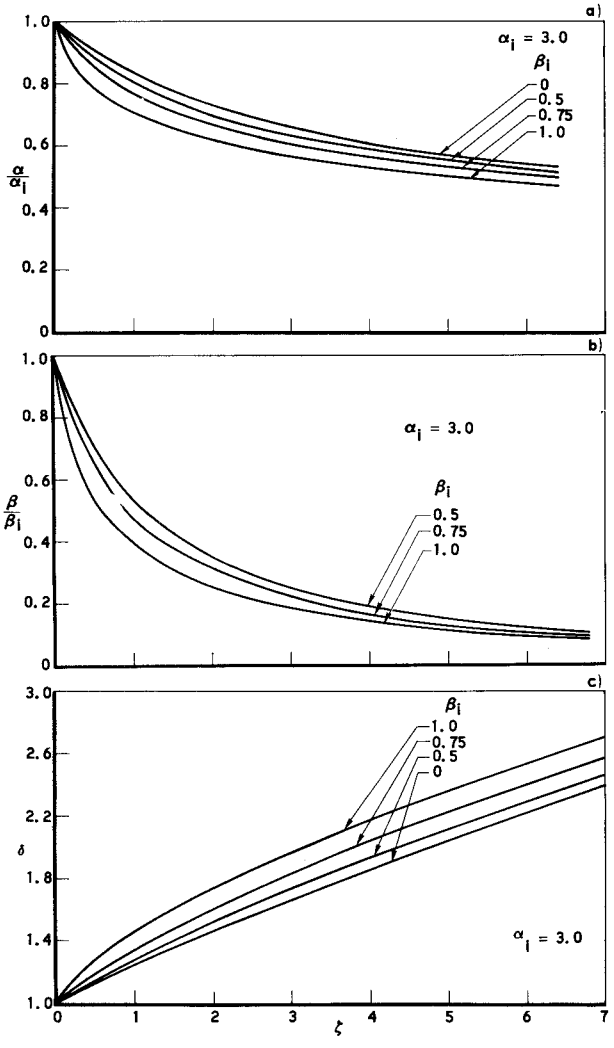

Fig. 5 Effect of swirl on jets: a) axial velocity on the axis; b) maximum circumferential velocity; c) flow boundary.

is obvious from Fig. 4 that for all these cases the intersection of the CP and ϕ lines will move away from α_d, β_d, towards $\alpha = 1$, $\beta = 0$. We thus see that these initial values of α_i, β_i will result in a continuous solution which satisfies the proper conditions at the downstream infinity. Typical examples of such solutions for $\alpha_i = 3$ and various values of β_i are shown in Figs. 5a–c. As may be seen in Figs. 5a and 5b, the axial and the circumferential velocities of the jet steadily decrease, with the swirling motion dissipating much faster than the axial velocity excess. Furthermore, Fig. 5c shows that at a fixed ζ the increase of the initial swirl causes the jet to expand and this, in line with the conservation of the angular momentum, enhances the dissipation of the swirling component (Fig. 5b). As seen in Fig. 5a, the increasing swirl also enhances the dissipation of the axial velocity excess. Thus Figs. 5a–c clearly show that the swirling jets are affected by increasing initial swirl in exactly the opposite way from swirling wakes and vortex cores. Since, for large r, the circulation of the swirling wakes, as well as the swirling jets, is diminishing, it is obvious that this difference in their behavior cannot be attributed to Rayleigh's rotational instability which some researchers[21–23] have suggested†† as a cause for the increased expansion (and thus entrainment) of swirling jets. It is also obvious that this difference cannot be attributed to any changes in turbulent eddy diffusivity[22,23] because ν_t could, at most, affect the relation between ζ and z but not $\alpha(\zeta)$, $\beta(\zeta)$, and $\delta(\zeta)$.

As already mentioned, the circumferential velocity of swirling jets dissipates much faster than their axial velocity excess. Thus far downstream, where the swirling flow is nearly dissipated, the swirling jets tend to behave like the nonswirling jets. The closed-form solution for nonswirling jets [Eqs. (7) and (8)] is also plotted in Figs. 5a and 5c. As may be seen from these figures, the effects of swirl disappear much faster in jets than in wakes.

Finally, it may again be noted from Fig. 4 that fixed β_i and decreasing α_i will yield qualitatively similar results to those shown in Figs. 5a–c for fixed α_i and increasing β_i. Thus for a fixed initial swirl and at a fixed axial position, with decreasing axial velocity we may expect the swirling jets to expand, but the swirling wakes to contract. These examples show that swirling jets behave quite differently from swirling wakes and vortex cores and that even for continuous solutions one should be cognizant of these entirely different characteristics.

Solutions with Modified Initial Conditions

When at any α_i, $\beta_i > \beta_d$ (say $\alpha_i = 2$, $\beta_i = 0.9$ on the $\phi = -0.6$ line), Fig. 4 shows that starting at these conditions the solution cannot proceed along the corresponding ϕ line towards $\alpha = 1$, $\beta = 0$ because between α_i, β_i and α_d, β_d CP would have to decrease in the downstream direction. Thus, starting at these initial conditions, the continuous solution can only move away from $\alpha = 1$, $\beta = 0$. However, when $P_{o,i} > 1$ (e.g., $CP_i < 0$), Fig. 4 also shows that the CP_i line will again intersect our ϕ line on the other side of the tangency point (for $\phi = -0.6$ at $\alpha = 1.25$, $\beta = 0.14$) so that starting at that intersection the solution can readily proceed to $\alpha = 1$, $\beta = 0$. Since all of our conservation laws are observed during such a process, we see that when $\beta_i > \beta_d$ and $P_{o,i} > 1$, the swirling jet solutions which properly satisfy the conditions at the downstream infinity may be approximated by crossing over along constant $P_{o,i}$ line to a new set of initial conditions from which regular, continuous solutions are obtainable.[16] Typically, such a crossover, right at the origin of the swirling jet, results in a sudden enlargement of the jet boundary and a sudden decrease of the axial and circumferential velocities.

For $P_{o,i} < 1$, the CP_i line cannot intersect its corresponding ϕ line and the previously described crossovers are no longer possible. Thus for such cases even approximate jet solutions cannot be found. However in reality, as will be seen later, these effects for $P_{o,i}$ equal to or smaller than unity, do not occur and the failure of the present method to properly describe the flow may be traced to the assumed axial velocity profiles which, for jets, were constrained to be only convex on the axis.

Still Surroundings

Normalizing α and β by w_{oi} instead of W, e.g., setting $\alpha = w_o/w_{oi}$, $\beta = V/w_{oi}$, $Re = (\bar{w}_o\bar{\delta}/\bar{\nu})_i$, and taking the limit as $W \to 0$, one obtains $w_{rr}(0) = -12w_{oi}\alpha/a$, $W^2F_1 = K_{12}w_{oi}{}^2\alpha^2$ and $WF_2 = K_{21}w_{oi}\alpha$. These simplify the previously derived expressions so that Eq. (4) may now be written as

$$K_{12}\alpha^2 + 0.5C_3\beta^2 - \phi(K_{21}\alpha\beta)^{2/3} = 0 \tag{9}$$

from which the lines of constant ϕ may readily be computed. However, since α_i must now always be unity,‡‡ therefore ϕ is directly related to β_i[16] and these lines may be more conveniently denoted by the value of their intial swirl. This was done in Fig. 6 where such lines of constant β_i are shown together with the lines of constant $CP = (1 - P_o)/w_{oi}{}^2$. As may be seen from this figure, all of the β_i lines now pass through the origin and the $CP = 0$ line is straight [given by $\alpha = \beta(2C_6)^{1/2}$]. Furthermore, the condition for the tangency of the β_i lines and the P_o lines can be shown to yield now $\alpha_d = 2.243\beta_d$, which again is a straight line through the origin.

Since the point $\alpha = 0$, $\beta = 0$ represents the proper conditions at the downstream infinity, one immediately sees, by examining Fig. 6, that the behavior of swirling jets is qualitatively unaffected by the axial motion of their surroundings. For, just as previously, when $\beta_i < \beta_d \sim 0.45$ they have a continuous solution, while for $0.45 < \beta_i < 0.56$ they require an adjustment of the initial conditions. Also for $\beta_i > 0.56$ (e.g., $P_{oi} < 1$), no solutions exist.

To carry out the integration along a constant β_i line we define the local swirl $\sigma \equiv \beta/\alpha$ (so that $0 \leqq \sigma \leqq \beta_i$) which when substituted into Eq. (9) and simplified form of Eq. (3b) with $\theta_2 \equiv k^2 - \sigma^2$ and $k = (-2K_{12}/C_3)^{1/2}$, yields

$$\alpha = (\sigma/\sigma_i)(\theta_{2i}/\theta_2)^{3/2}; \quad \beta = \sigma\alpha; \quad \delta = (\sigma_i/\sigma)(\theta_2/\theta_{2i}) \tag{10}$$

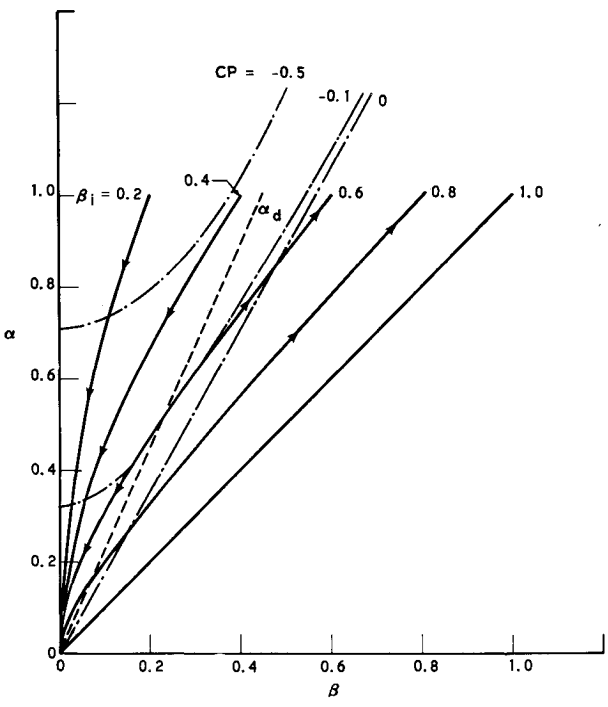

Fig. 6 Phase plane for jets in still surroundings.

†† It is pertinent to note that Rayleigh proposed his criterion for purely rotational flows and not those having both circumferential and axial velocities.

‡‡ This does not mean that the solution must be initiated at the jet's origin. Any point downstream from the origin with its corresponding value of $w_o = w_{oi}$ can serve as the initial point, providing care is taken to properly adjust $\phi = \kappa_1/(\kappa_2 w_{oi})^{2/3}$ or β_i.

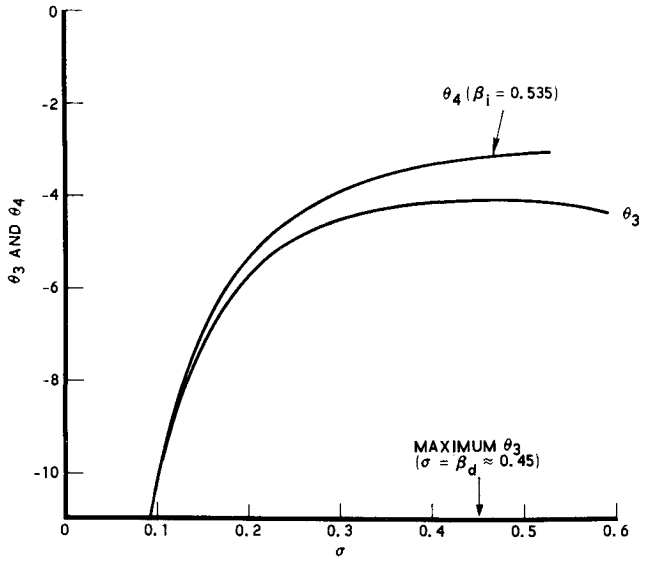

Fig. 7 Functions relating axial distance and local swirl for jets in still surroundings.

Furthermore Eq. (3d), after appropriate simplification, may now be integrated in a closed form with $\zeta_i = 0$ and

$$\theta_3 \equiv -\{[\theta_2{}^{1/2}(1-C_6\sigma^2)/k\sigma]+[5kC_6-(2/k)]\arcsin(\sigma/k)\}$$

to give

$$\zeta = k\sigma_i(\theta_{3i}-\theta_3)/(\theta_{2i})^{1/2} \tag{11}$$

Function θ_3 is shown in Fig. 7 and has a maximum at $\sigma \approx 0.45$ so that for $\beta_i > 0.45$, an adjustment of initial conditions must be made if Eq. (11) is to give $\zeta > 0$. The adjusted, initial value of $\sigma_i(\neq\beta_i)$ may be obtained by finding that σ_i for which $CP = CP_i$. This leads to a cubic equation in $\sigma_i{}^2$ whose real root gives the desired answer. Of course, for $\beta_i > [1/(2C_6)^{1/2}]$ the method fails. An example of the so obtained solution will be given below. Also, for small β_i Eqs. (10) and (11) may be simplified to

$$\alpha = 1/(1+\zeta); \quad \beta = \beta_i/(1+\zeta)^2; \quad \delta = 1+\zeta \tag{12}$$

so that for large ζ, α, and β are seen to behave like those of a nonswirling jet in still surroundings.§§ It is thus apparent that when the surroundings of the swirling jet are in axial motion its expansion is not as rapid [$\delta \sim (\zeta)^{1/2}$, see Eq. (8)] as it is when the surroundings are at standstill.

The variations indicated by Eqs. (12) are in good agreement with the results previously obtained by Loitsyanskii[2] who "ab initio" assumed a linear dependence between δ and ζ and then obtained his axial and circumferential velocity profiles in form of expansions whose zero-order terms represented the flow without swirl and which led to infinite velocities at the origin. The present results are also in agreement with the results of Steiger and Bloom[9] and Görtler[3] who neglected the radial variation of static pressure thus restricting the applicability of their answers to flows with very small swirl.

Of greater interest, however, is the comparison with the solution of Narrain and Uberoi[10] specifically constructed for turbulent flow. To obtain their answer Narrain and Uberoi used momentum-integral equations but instead of the condition on the axis, which involves ν_t, they substituted an approximate volume-flow entrainment equation, applicable at the boundary of the jet and whose swirl-dependent entrainment coefficient they obtained by use of the energy-integral equation. Examining their work we note that, by setting $k = N_1$ [using the nomenclature of Ref. 10: $N_1 \equiv 1/(2ak_1)^{1/2}$; $N_2 \equiv c_2$; $N_3 \equiv c_3$; $N_4 \equiv 1/(4\alpha k_1 a^2)$], their equations are also solvable in closed form and, in particular, we again obtain α, β, and δ from Eqs. (10) while, taking $z_i = 0$ and $\theta_4 \equiv -[(1/\sigma)+N_2\sigma+(N_3\sigma^3/3)]$, the axial coordinate is given by

§§ For jets in still surroundings Eqs. (7) simplify to $\alpha\delta = 1$; $a\alpha' = -1$ whose solution is also given by Eqs. (12).

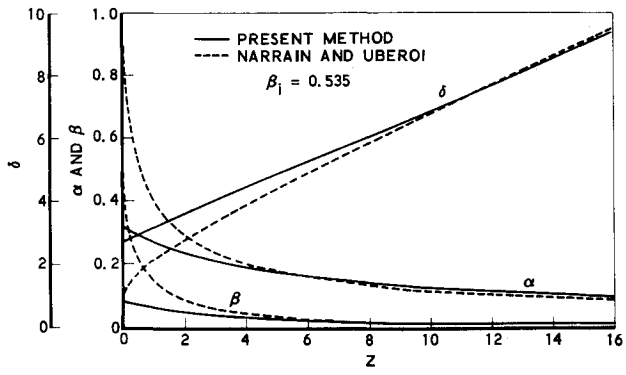

Fig. 8 Comparison with the solution of Narrain and Uberoi.[10]

$$z = \sigma_i N_4(\theta_{4i}-\theta_4)/\theta_{2i} \tag{13}$$

Function θ_4 for $\beta_i = 0.535$ is shown in Fig. 7. Its behavior and values for other β_i are not too different from that shown there. From Fig. 7 we find that the greatest difference between θ_3 and θ_4 occurs for largest σ and therefore we may expect this difference to be most influential for largest β_i. Thus a comparison with the results of Ref. 10 at $\beta_i = 0.535$ was deemed to be most critical. It should be noted that this value of β_i requires an adjustment of the initial conditions so that such a comparison has the additional advantage of showing the nature of the so obtained solutions. To carry it out one needs to specify $\nu_t = 1/Re_t$. This may be done by requiring in the limit, as $\sigma \to 0$, that z for both solutions be the same. For $\beta_i = 0.535$ this gives $\nu_t = 0.0125$. The so matched solutions are shown in Fig. 8. As may be seen from that figure, for all $z > 5$, the present solution (for α, β, and δ) and the solution of Narrain and Uberoi are within 10% of each other. Similar computations carried out at lower values of β_i show, as expected, an even better agreement. We thus see that, when matched at large z, the two solutions give nearly the same answers.

Experimental Validation

As mentioned in the Introduction, only one[11] experimental investigation of swirling wakes in axially moving surroundings exists. The results of this investigation show that, at any given axial position, increasing swirl tends to decrease the difference between the axial velocity on the axis and the freestream velocity. This behavior, while in agreement with that described by the present method for jets (see Fig. 5a), is in direct contradiction of that expected for wakes (Fig. 2a). It is unfortunate therefore that the investigation reported in Ref. 11 was somewhat incomplete, and in particular did not include measurements of flow direction so that one cannot be sure of the validity of its results.

The other experimental data that the present results may be compared with are those obtained for jets in still surroundings. All of this data is for turbulent flow so that before attempting a comparison, one must know how the turbulent eddy diffusivity is affected by swirl. Fortunately, for jets in still surroundings, one may easily determine this from the slope of the volume-flow curves.

In particular, normalizing the volume-flow by dividing it by its initial value $M \equiv \bar{M}/\bar{M}_i = \alpha a$, one may show that, in the limit as $\sigma \to 0$, the slope of the volume-flow curves M' is unity and therefore $\nu_t = 0.0417\ (dM/dz)$. The constancy of dM/dz is well confirmed, even at low z/d (with d being the jet's nozzle diameter), by the data of Ref. 5 and the so determined ν_t is plotted in Fig. 9. Also shown is the single data point of Rose (Ref. 6)¶¶ a number of values for nonswirling jet $\nu_{t,n}$ obtained

¶¶ Rose computed $\bar{\nu}_t$ and $\bar{\nu}_{t,n}$ by using an expression for the derivative of volume-flow from Ref. 2. At $z/d = 3.06$, his $\bar{\nu}_t$ gives $\nu_t = 0.0093$.

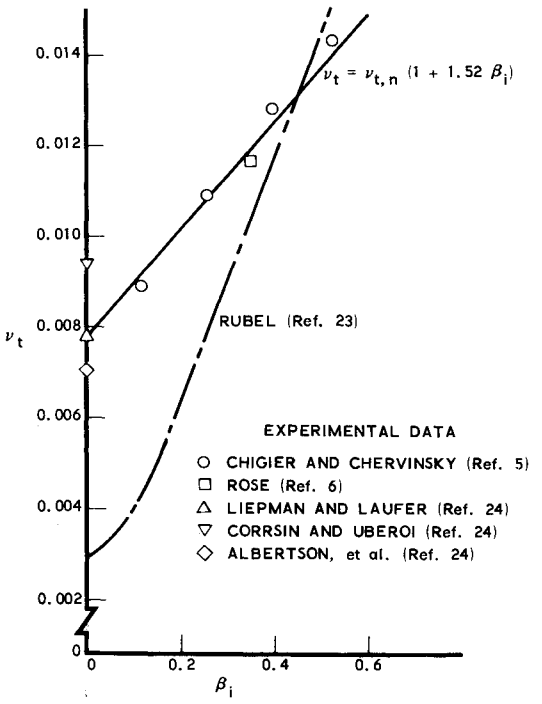

Fig. 9 Effect of swirl on turbulent diffusivity.

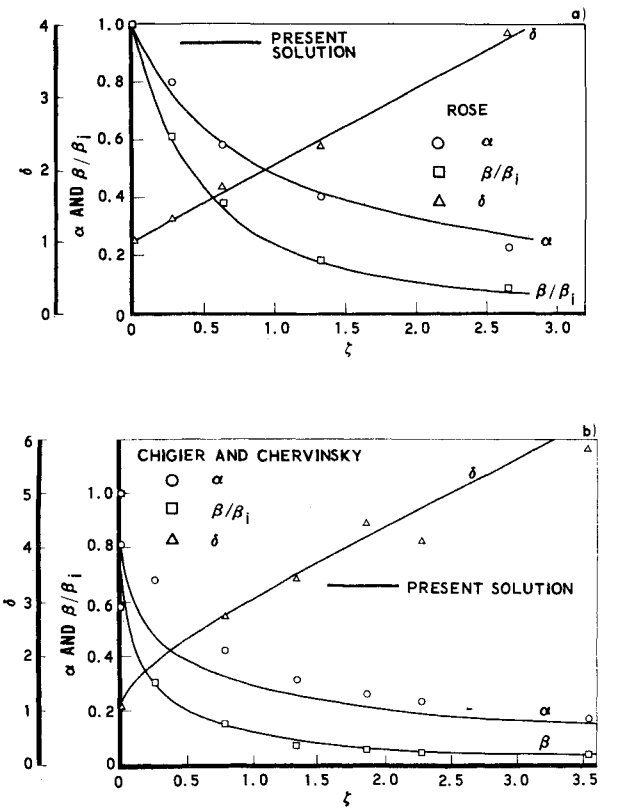

Fig. 10 Comparison with experimental data: a) at low swirl (Rose[6]); b) at medium swirl (Chigier and Chervinsky[5]).

by various investigators[24] and the expression of Rubel.[23] As may be seen, all of the experimental data appear to be reasonably well correlated by $\nu_t = \nu_{t,n}(1+1.52\beta_i)$ which strongly supports Bradshaw's[22] concept of a linear correction for the effect of extra rates of strain on the turbulence structure. This correlation also agrees with the ν_t that was previously used for matching the entrainment solution of Ref. 10 at $\beta_i = 0.535$. Rubel's nonlinear formula, which predicts a much greater effect of swirl on ν_t, tends to give values which are much too low at small β_i and in particular completely misses the nonswirling $\nu_{t,n}$.

We are now able to test the validity of the present method at low swirl against the data of Rose.[6] Starting the solution at $z/d = 3.06$ where $\beta_i = 0.15$ we obtain the results shown in Fig. 10a. This figure shows that the present method describes turbulent flow behavior which is very well confirmed by the measurements of Rose.

To obtain an insight into flow changes which may be occurring when the swirl is high enough to require an adjustment of the initial conditions, a comparison with the data of Ref. 5, taken nominally at $\beta_i = 0.53$, was attempted. Although Chigier and Chervinsky do not indicate any sudden changes in flow conditions near the jet's nozzle, their data points were not taken at sufficiently small intervals of z to be sure that this was really so. Using therefore the actual conditions measured near the nozzle exit at $z/d = 0.2$ (e.g., $\beta_i = 0.47$, $Re_t = 73$) and assuming that the adjustment process is completed just ahead of $z/d = 1$ (so that $\zeta = 0$ at $z/d = 1$), one obtains a solution which is compared with the experimental data of Ref. 5 in Fig. 10b. As may be seen from that figure the so computed solution agrees quite well with the experimental measurements of β and δ but, with the exception of the point at $\zeta = 0$, tends to underestimate α.

At still higher values of swirl ($\beta_i = 0.68$), the experimental data of Ref. 5 shows that immediately outside the exit nozzle (e.g., at $z/d = 0.2$) not only does the jet suddenly increase its cross-sectional area, but also the axial velocity is locally, drastically decelerated, so that the axial velocity profile reverses its curvature on the axis, developing a concavity which slowly disappears as the flow proceeds downstream. This concavity gets stronger with increasing swirl so that at the nominal $\beta_i = 0.73$ the swirling jet starts with a reversed flow on the axis.

In seeking the analytical explanation of this behavior, we note from Fig. 6 that $P_{oi} < 1$ for $\beta_i > 0.56$ so that as the flow proceeds, P_o must increase in the downstream direction. But according to Eq. (1d) this requires that $w_{rr}(0)$ be positive and the velocity profile be concave there. We thus see that the experimental data of Ref. 5 strongly supports the validity of the on-axis condition *for turbulent flow* and also explains why the present solution, which, because of the assumed axial velocity profile, is incapable of changing the sign of $w_{rr}(0)$, must fail when $P_{oi} < 1$.

Since similar considerations will also apply when the swirling jet issues into a moving stream, we may conclude that, in general, the swirling jets will originate with concave axial velocity profiles and possibly reversed flow near the axis when the initial swirl is high enough to lower the axis total pressure to about its value in their surroundings.

Summary of Findings

1) Though the equations for swirling wakes and swirling jets are not always integrable in a closed form, the course of their solutions is easily visualized in a phase plane. This permits the determination of their behavior near the discontinuities and also allows discernment of those solutions which are physically realistic, that is, lead to the proper conditions at the downstream infinity.

2) At a given axial position, increasing initial swirl or decreasing initial axial velocity, affects the swirling wakes in an opposite way from the swirling jets. Thus while these changes tend to make the wakes more slender and delay the dissipation of the circumferential velocity and the axial velocity deficiency, in jets; they tend to expand the flow and enhance the dissipation of the circumferential velocity and the axial velocity excess. These differences arise as a consequence of the conservation laws and not because of rotational instability or any increase in turbulent eddy diffusivity.

3) In swirling wakes and in swirling jets the circumferential velocity tends to dissipate faster than the axial velocity excess (or deficiency). Thus, far downstream, both swirling wakes and swirling jets tend to behave like the nonswirling ones.

4) When the surroundings of swirling jets (or wakes) are in axial motion they do not expand as rapidly as they do when their surroundings are at a standstill.

5) The behavior of solutions near discontinuities indicates that the asymmetric, spiral breakdown, which has been observed in vortex cores, is likely to occur in a similar form also in wakes whose relative flow force deficiency and initial swirl are sufficiently high ($\phi > 0.77$ and $\beta_i > 0.64$), but only when the appropriate α_d and β_d are reached.

6) In jets, though the solutions have discontinuities, the experiments of Chigier and Chervinsky[5] show that these discontinuities are not indicative of the asymmetric, spiral breakdown but, because of constraints imposed by the present method on the assumed axial velocity profiles, cause only analytical difficulties. The conditions producing these difficulties indicate that swirling jets begin developing initially-concave, axial velocity profiles on the axis (and, eventually, reversed flow) when the swirl is high enough to lower the initial total pressure on the axis to about its value in the surroundings.

7) The present method is in full agreement with the analyses of swirling wake by Gartshore[15] and by Steiger and Bloom.[13] It is also in very good agreement with the various analyses of swirling jets in still surroundings and in particular with the properly matched entrainment coefficient method, specifically devised for turbulent flow, by Narrain and Uberoi.[10]

8) For turbulent swirling jets in still surroundings and at low swirl, the present method is very well validated by the experimental data of Rose.[6] At moderate swirl, the comparison between the present method and the experimental data of Chigier and Chervinsky[5] indicates good agreement of the circumferential velocities and jet diameters, but a slight, though consistent, underestimate of the axial velocities.

9) The on-axis condition gives results which are well supported by the experimental data of Chigier and Chervinsky[5] for very strongly swirling and dissimilarly behaving turbulent jets in still surroundings.

10) For swirling jets in still surroundings, a convenient technique for the experimental determination of the effect of the initial swirl on the turbulent eddy diffusivity shows the correction factor to be nearly linear, as postulated by Bradshaw,[22] but much weaker than indicated by Rubel.[23]

Appendix: Constants and Coefficients

Define

$$C_i \equiv \int_0^1 f_1^l f_2^m \eta^t \, d\eta$$

Then the integration yields the values of C_i given in Table 1.

Table 1 Constants C_i

i	l	m	t	C_i
1	1	0	1	4/10
2	2	0	1	111/315
3	0	2	1	8192/76545
4	1	1	2	1376/31185
5	0	1	2	64/945
6	0	2	−1	8192/5103

Using these values of C_i we can obtain the values of the coefficients K_{ji} given in Table 2.

Table 2 Coefficients K_{ji}

j \ i	0	1	2
1	$C_1 - C_2$	$0.5 - 3C_1 + 2C_2$	$2C_1 - C_2 - 0.5$
2	C_4	$C_5 - C_4$	0

References

[1] Mager, A., "Dissipation and Breakdown of a Wing-Tip Vortex," *Journal of Fluid Mechanics*, Vol. 55, Pt. 4, 1972, pp. 609–628.

[2] Loitsyanskii, L. G., "The Propagation of a Twisted Jet in an Unbounded Space Filled with the same Fluid," *Prikladnaya Matematika i Mekhanika*, Vol. 17, 1953, pp. 3–16.

[3] Görtler, H., "Decay of Swirl in an Axially Symmetrical Jet Far from the Orifice," *Revista Matematica Hispano Americanas*, Ser. 4, Vol. 14, 1954, pp. 143–178.

[4] Lee, S. L., "Axisymmetrical Turbulent Swirling Jet," *Journal of Applied Mechanics*, Vol. 32, Ser. E, No. 2, June 1965, pp. 258–262.

[5] Chigier, N. A. and Chervinsky, A., "Experimental and Theoretical Study of Turbulent Swirling Jets Issuing from a Round Orifice," *Israel Journal of Technology*, Vol. 4, No. 1, 1966, pp. 44–54.

[6] Rose, W. G., "A Swirling Round Turbulent Jet," *Journal of Applied Mechanics*, 1962, pp. 615–625.

[7] Iserland, K., "Untersuchungen über die Umlenkung eines freien Luftstrahls mit Hilfe von Drall," Mitteilungen aus dem Institut für Aerodynamik an der Eidgenössischen Technischen Hochschule in Zürich, Nr. 25, 1958.

[8] Mathur, M. L. and Maccallum, N. R. L., "Swirling Air Jets Issuing from Vane Swirlers. Part 1: Free Jets," *Journal of the Institute of Fuel*, Vol. 40, No. 316, May 1967, pp. 214–225.

[9] Steiger, M. H. and Bloom, M. H., "Axially Symmetric Free Mixing with Swirl," PIBAL Rept. 628, Nov. 1960, Polytechnic Institute of Brooklyn, Brooklyn, N.Y.

[10] Narrain, J. P. and Uberoi, M. S., "The Swirling Turbulent Plume," ASME Paper 73-WA/APM-23, Detroit, Michigan, 1973.

[11] Liu, C. Y., "Wake of an Axially Symmetrical Body with Spinning," *Proceedings of the Ninth International Symposium on Space Technology and Science*, Tokyo University and Japanese Rocket Society and 56 Companies, Tokyo, 1971, pp. 373–378.

[12] Chervinsky, A. and Lorenz, D., "Decay of Turbulent Axisymmetrical Free Flows with Rotation," *Transactions of the ASME*, Ser. E: Journal of Applied Mechanics, Vol. 34, 1967, pp. 806–812.

[13] Steiger, M. H. and Bloom, M. H., "Axially Symmetric Laminar Free Mixing with Large Swirl," PIBAL Rept. 626, Jan. 1961, Polytechnic Institute of Brooklyn, Brooklyn, N.Y.

[14] Gartshore, I. S., "Recent Work in Swirling Incompressible Flow," Aeronautical Rept. LR-343, NRC No. 6968, June 1962, National Research Council of Canada, Ottawa, Canada.

[15] Gartshore, I. S., "Some Numerical Solutions for the Viscous Core of an Irrotational Vortex," Aeronautical Rept. LR-378, NRC No. 7479, June 1963, National Research Council of Canada, Ottawa, Canada.

[16] Mager, A., "Swirling Jets and Wakes," AIAA Paper 74-35, Washington, D.C., 1974.

[17] Hall, M. G., "Vortex Breakdown," *Annual Review of Fluid Mechanics*, Vol. 4, Annual Review, Inc., Palo Alto, Calif., 1972, pp. 195–217.

[18] Sarpkaya, T., "On Stationary and Travelling Vortex Breakdowns," *Journal of Fluid Mechanics*, Vol. 45, 1971, pp. 545–559.

[19] Sarpkaya, T., "Effect of the Adverse Pressure Gradient on Vortex Breakdown," *AIAA Journal*, Vol. 12, No. 5, May 1974, pp. 602–607.

[20] Benjamin, T. B., "Theory of the Vortex Breakdown Phenomenon," *Journal of Fluid Mechanics*, Vol. 14, 1962, pp. 593–629.

[21] Emmons, H. W., Comments on paper "Aerodynamic Study of Turbulent Burning Free Jets with Swirl," by Chigier, N. A. and Chervinsky, A., *Eleventh Symposium on Combustion*, The Combustion Institute, Pittsburgh, Pa., 1967, pp. 497–498.

[22] Bradshaw, P., "Effects of Streamline Curvature on Turbulent Flow," AGARD-AG-169, 1973.

[23] Rubel, A., "Some Effects of Swirl on Turbulent Mixing and Combustion," CR-1956, 1972, NASA.

[24] Nielsen, J. N., Stahara, S. S., and Woolley, J. P., "A Study of Ingestion and Dispersion of Engine Exhaust Products in Trailing Vortex Systems," NEAR TR 54, 1973, Nielsen Engineering and Research, Inc., Mountain View, Calif.